

Published in final edited form as:

Biochem Pharmacol. 2011 November 1; 82(9): 1100–1109. doi:10.1016/j.bcp.2011.07.078.

Anti-cancer Effects of Novel Flavonoid Vicenin-2 as a Single Agent and in Synergistic Combination with Docetaxel in Prostate Cancer

Lokesh Dalasanur Nagaprashantha, Rit Vatsyayan, Jyotsana Singhal, Spence Fast, Rhonda Roby, Sanjay Awasthi, and Sharad S. Singhal*

Department of Molecular Biology and Immunology, University of North Texas Health Science Center, Fort Worth, TX 76107

Abstract

The present study was conducted to determine the efficacy of novel flavonoid vicenin-2 (VCN-2), an active constituent of the medicinal herb *Ocimum Sanctum Linn* or *Tulsi*, as a single agent and in combination with docetaxel (DTL) in carcinoma of prostate (CaP). VCN-2 effectively induced anti-proliferative, anti-angiogenic and pro-apoptotic effect in CaP cells (PC-3, DU-145 and LNCaP) irrespective of their androgen responsiveness or p53 status. VCN-2 inhibited EGFR/Akt/mTOR/ p70S6K pathway along with decreasing c-Myc, cyclin D1, cyclin B1, CDK4, PCNA and hTERT *in vitro*. VCN-2 reached a level of 2.6 ± 0.3 micromol/L in serum after oral administration in mice which reflected that VCN-2 is orally absorbed. The *i.v.* administration of docetaxel (DTL), current drug of choice in androgen-independent CaP, is associated with dose-limiting toxicities like febrile neutropenia which has lead to characterization of alternate routes of administration and potential combinatorial regimens. In this regard, VCN-2 in combination with DTL synergistically inhibited the growth of prostate tumors *in vivo* with a greater decrease in the levels of AR, pIGF1R, pAkt, PCNA, cyclin D1, Ki67, CD31, and increase in E-cadherin. VCN-2 has been investigated for radioprotection and anti-inflammatory properties. This is the first study on the anti-cancer effects of VCN-2. In conclusion, our investigations collectively provide strong evidence that VCN-2 is effective against CaP progression along with indicating that VCN-2 and DTL co-administration is more effective than either of the single agents in androgen-independent prostate cancer.

Keywords

Prostate cancer; vicenin-2; docetaxel; tumor xenografts

1. Introduction

Carcinoma of prostate (CaP) is one of the leading causes of male cancer deaths ranking only next to lung cancer in United States. The fact that 1 in 3 men develop prostatic intraepithelial neoplasia (PIN), an early event in the malignant transformation of prostate,

© 2011 Elsevier Inc. All rights reserved.

*Address correspondence to: Sharad S. Singhal., Associate Professor, Phone: 817-735-2236; Fax: 817-735-2118; sharad.singhal@unthsc.edu.

Publisher's Disclaimer: This is a PDF file of an unedited manuscript that has been accepted for publication. As a service to our customers we are providing this early version of the manuscript. The manuscript will undergo copyediting, typesetting, and review of the resulting proof before it is published in its final citable form. Please note that during the production process errors may be discovered which could affect the content, and all legal disclaimers that apply to the journal pertain.

and that 1 in 6 men develop CaP reflects the associated life-time risk for CaP. According to the latest available 1973-2008 surveillance data from national cancer institute (NCI), CaP is a highly incident malignancy in men with 2,276,112 prevalent cases and approximately 217,730 new CaP cases in the year 2010 [1]. The characteristic feature of incident tumors within the prostate is the “multifocality” and different clinical grades or “heterogeneity” [2]. This distinct feature of CaP translates every single clinical case into a set of prostate tumors with varying molecular complexity which in turn contributes to distinct invasive and metastatic properties [3-5].

The pathogenesis of CaP is marked by the initial onset of precancerous PIN followed by loss of basal lamina and transformation to locally invasive carcinoma which further progresses to metastatic CaP [6]. The activation of C-Myc and loss of tumor suppressor PTEN are two established and predominant genetic factors in the primary pathogenesis of CaP while concomitant loss of Rb and p53 are known to enhance the incidence of CaP [7-9]. The activation of growth factor cascades like EGFR and its downstream Akt and mTOR signaling plays a vital role in transducing the oncogene activated mitogenic and survival signals. The progression of CaP to androgen independence is associated with activation of IGF-1R, over-expression of anti-apoptotic proteins like Bcl2 along with loss of tumor suppressor E-cadherin [10-12]. Given the elderly age group affected by CaP, the potential candidate chemopreventive compounds need to be safe for consumption till later years of life and should effectively target the critical nodes of signaling networks of particular relevance to the pathogenesis and progression of CaP.

“*Ocimum Sanctum* Linn (*OSL*; family: *Lamiaceae*)” also known as “Holy basil” and “*Tulsi*”, is an extensively cultivated Indian herb which is known for its medicinal properties in the Indian subcontinent with a safe record of human consumption from thousands of years [13]. *OSL* constituents have been known for their anti-oxidant, anti-inflammatory and anti-diabetic properties [13,14]. Oxidative stress is a well established cause in the initiation and progression of cancers [15]. Anti-oxidant and anti-inflammatory compounds like cyclooxygenase-2 inhibitors, natural compounds like silibinin and other flavonoids are being intensely investigated for prostate cancer interventions [16,17]. *OSL* has been investigated for its chemopreventive properties in DMBA induced oral cancer [18].

Currently, Docetaxel (DTL) is administered *i.v.* at a dose of 60-100 mg/m² once every three weeks in clinical practice. The dose-limiting adverse effect of DTL is febrile neutropenia and associated myelotoxicity [19]. Even anemia and non-febrile neutropenia, which result in approximately 41% and 67% of cases of DTL administration can severely affect the quality of life and consequent survival in elderly patients, given that many CaP patients have extensive comorbidities like diabetes mellitus and age related decline in immune function. Myelotoxicity or bone marrow toxicity results in direct and high level of exposure to bolus dose of DTL which is typical with *i.v.* route of administration. Though, some of the previous studies focused on trying to switch from three week to weekly doses with moderate dosage reduction, still the adverse effects were substantial like hyperlacrimation, skin- and nail-toxicity and negatively affects quality of life [19]. Repeated oral administration of drug leads to maintenance of steady state levels of drug with relatively less chances of high dose exposure typical of single high *i.v.* dose of DTL. Many investigations have focused on the combinatorial therapies, but few studies have been carried out on alternate routes of administration of DTL [19-22]. In this regard, we first tested the anti-cancer potential of Vicenin-2 (VCN-2), an active constituent of *OSL*, in CaP followed by investigating the impact of VCN-2 alone and in combination with DTL *in vivo* mice xenograft models of CaP by oral gavage. Our studies provided strong evidence to the tumor selective anti-proliferative, anti-angiogenic, pro-apoptotic and anti-metastatic properties of VCN-2 and its synergistic inhibitory effect with DTL along with elucidating differential regulation of

significant signaling proteins that mediate critical nodes of transformation, maintenance of limitless replicative potential, androgen-dependent progression of primary CaP as well as emergence of androgen-independent CaP.

2. Materials and Methods

2.1. Reagents

MTT and luteolin (purity >98%) were obtained from Sigma (St Louis, MO). Vicenin-2 and orientin (purity >98% by HPLC; solubility in DMSO) were purchased from Quality Photochemical, Edison, NJ. For *in vitro* studies, VCN-2 stock solution was prepared in DMSO, and further diluted into medium as a working solution (final concentration of DMSO in the experiment is < 0.001%). For *in vivo* studies, VCN-2 powder was suspended into corn oil for oral feeding by gavage. Docetaxel was in saline, provided by Dr. Sanjay Awasthi, M.D., Medical Oncologist and Professor, Texas Cancer Center, Medical Center of Arlington, Arlington, TX. PARP, Bcl2, Bax, fibronectin, E-cadherin, cyclin B1, cyclin D1, CDK4, PCNA, hTERT, EGFR, pEGFR (Y¹⁰⁶⁸), Akt, pAkt (S⁴⁷³), GAPDH, P70S6K, p-P70S6K (S²⁴⁰⁻²⁴⁴), C-Myc, Rb, pRb (S⁷⁸⁰), p53, p21, β -actin, Ki67, CD31, IGF-1R, and pIGF-1R (Y¹¹³¹) antibodies were purchased from Santa Cruz Biotechnology (Columbus, OH), Upstate Cell Signaling (Lake Placid, NY), and Cell Signaling Technologies (Danvers, MA). ELISA kit for VEGF-expression was procured from R&D Systems (Minneapolis, MN). APO LOGIXTM carboxyfluorescein (FAM) caspase detection kit was purchased from Cell Technology (Minneapolis, MN). Matrigel was procured from BD Biosciences (San Jose, CA). TUNEL fluorescence and avidin/biotin complex (ABC) detection kits were purchased from Promega (Madison, WI) and Vector (Burlingame, CA), respectively.

2.2. Cell Lines and Cultures

Human prostate carcinoma LNCaP (androgen-dependent), PC-3 & DU-145 (androgen-independent) cell lines were purchased from the American Type Culture Collection (ATCC, Manassas, VA) in April 2009. The authentication of cell lines was done by analyzing fifteen different human short tandem repeat (STR) (done by Center for Investigative Genetics core facility at UNTHSC, Fort Worth, TX) to test for interspecies contamination. The cell lines were last tested in December 2010. The normal human prostate epithelial cells (PREC) were a kind gift from Prof Sanjay Gupta (Case Western Reserve University, Cleveland, OH). All cells, except PREC, were cultured at 37 °C in a humidified atmosphere of 5 % CO₂ in RPMI-1640 medium supplemented with 10 % FBS and 1% P/S solution. PREC cells were maintained in K-SFM medium with supplementation provided by the vendor (Invitrogen, Carlsbad, CA). All the cells were also tested for *Mycoplasma* once every 3 months.

2.3. Colony forming assay

Cell survival was evaluated using a standard colony-forming assay. 1×10^5 cells / ml were incubated with VCN-2 (50 μ M) for 24 h, and aliquots of 50 or 100 μ l were added to 60-mm size Petri dishes containing 4 ml culture medium. After 10 days, adherent colonies were fixed, stained with 0.5% methylene blue for 30 min and counted using the Innotech Alpha-Imager HP [23].

2.4. In situ caspase-3 cleavage assay

Detection of active caspase-3 in live cell cultures was performed using an APO LOGIXTM carboxyfluorescein (FAM) caspase detection kit (Cell Technology). The kit detects active caspase-3 in living cells through FAM-labeled DEVD fluoromethyl ketone (FMK), which irreversibly binds to active caspase-3. The inhibitor is cell permeable and noncytotoxic. The assay was performed according to manufacturer's instructions [24].

2.5. Apoptosis assays

For apoptosis assays, 1×10^5 cells were grown on the cover-slips for ~12 h followed by treatment with VCN-2 (50 μ M) for 24 h. For annexin V staining, after VCN-2 treatment, cells were washed with ice-cold PBS, treated with 100 μ l of annexin-binding buffer (10 mM HEPES, 140 mM NaCl and 2.5 mM CaCl_2 , pH 7.4) containing 10 μ l of annexin V conjugate and incubated for 15 min at room temperature. The cells were washed with the annexin-binding buffer and mounted on the slide. Fluorescence micrographs were taken using Zeiss LSM 510 META (Germany) laser-scanning fluorescence microscope at 400 x magnifications [25]. In TUNEL assay, apoptosis was determined by the labeling of DNA fragments with terminal deoxynucleotidyl-transferase dUTP nick-end labeling (TUNEL) using Promega fluorescence apoptosis detection system. Slides were analyzed under a fluorescence microscope using a standard fluorescein filter set to view the green fluorescence at 520 nm and red fluorescence of propidium iodide at >620 nm [26]. For Hoechst staining, the cover-slips were fixed in 95% alcohol for 15 min and incubated in a Hoechst 33342 staining solution (3 μ l of 10 mg/ml) in 10 ml PBS for 20 min. The stained cells were examined under a fluorescence microscope for chromatin aggregation which is a hallmark of apoptosis [27].

2.6. Aortic ring assay

Aortic ring assay was performed as described by Yi et al [28]. Aortas were dissected from mice and were cut into ~1.5-mm-long rings and rinsed with endothelial cell-based medium. The 48-well plates were initially covered with 100 μ L of Matrigel at 4°C and then incubated at 37°C at 5% CO_2 for 30 min. The aortic rings were placed on the Matrigel in the 48-well plates and covered with additional 100 μ L of Matrigel. The aortic artery rings were cultured in 1.5 mL of ECGM without serum for 24 h, and then the medium was replaced with 1.5 mL of ECGM with or without 50 μ M of VCN-2. The medium was changed on 2nd day. On 4th day after starting treatment, the micro-vessel growth was quantified by taking photographs with Olympus Provis AX70 microscope.

2.7. In vitro migration assay

Cell migration was determined using a wound healing assay. 2×10^4 LNCaP and PC-3 cells were seeded in 6-well plates to reach 100% confluence within 24 h and then treated with 10 μ M mitomycin C for 2 h. Subsequently, a similarly sized scratch was made with a 200 μ L pipette tip across the center of each well and immediately imaged at baseline and then at 24 h in control and VCN-2 treated groups by using an Olympus Provis AX70 microscope. The rate of cell migration was determined by comparing the sizes of scratch area using Image J software.

2.9. Flow cytometry analysis of cell cycle regulation

2×10^5 cells were treated with VCN-2 (50 μ M) for 18 h at 37 °C. After treatment, floating and adherent cells were collected, washed with PBS, and fixed with 70 % ethanol. On the day of flow analysis, cell suspensions were centrifuged; counted and same numbers of cells were resuspended in 500 μ l PBS in flow cytometry tubes. Cells were then incubated with 2.5 μ l of RNase (stock 20 mg/ml) at 37 °C for 30 min after which they were treated with 10 μ l of propidium iodide (stock 1mg/ml) solution and then incubated at room temperature for 30 min in the dark. The stained cells were analyzed using the Beckman Coulter Cytomics FC500, Flow Cytometry Analyzer. Results were processed using CXP2.2 analysis software from Beckman Coulter.

2.10. Ingenuity Pathway Analysis (IPA)

The IPA was performed using Uniprot/swiss prot IDs of proteins and ratios obtained from the densitometric analyses of Western-blot after VCN-2 treatment using the IPA (Ingenuity Systems, Redwood City, CA) to elucidate differential regulation of signaling pathways and networks.

2.11. In vivo xenograft studies

Hsd: Athymic nude nu/nu mice were obtained from Harlan, Indianapolis, IN. All animal experiments were carried out in accordance with and approved by University of North Texas Health Science Center (UNTHSC) Institutional Animal Care and Use Committee (IACUC) approved protocol. Twenty 11-week-old mice were divided into four groups of 5 animals [(For treatment with (i) corn oil (vehicle), (ii) vicenin-2 (1 mg/kg b.w.), (iii) docetaxel (0.01 mg/kg b.w.), and (iv) vicenin-2 + docetaxel]. All 20 animals were injected with 2×10^6 prostate cancer cells (PC3) suspensions in 100 μ l of PBS, subcutaneously into one flank of each nu/nu nude mouse. At the same time, animals were randomized treatment groups as indicated in the figures (**Fig 5 and Supplementary Fig 2**). Treatment was started 10 days after the PC3 cells implantation to see palpable tumor growth. Treatment consisted of vicenin-2 (1 mg/kg b.w.) or docetaxel (0.01 mg/kg b.w.) or both vicenin-2 and docetaxel, in 100 μ l corn oil by oral gavage alternate day. Control groups were treated with 100 μ l corn oil by oral gavage alternate day. Animals were examined daily for signs of tumor growth. Tumors were measured in two dimensions using calipers. Photographs of animals were taken at day 1, day 10, day 20, day 40, and day 60 after subcutaneous injection, are shown for all groups. Photographs of tumors were also taken at day 60.

2.12. Histopathological examination of tumors for angiogenic, proliferative and differentiation markers

Tumors from PC3 mice xenografts (control and VCN-2 treated) were harvested on day 60. Tumor samples fixed in buffered formalin for 12 h were processed conventionally for paraffin-embedded tumor sections (5 μ m thick). Hematoxylin and Eosin (H&E) staining was performed on paraffin-embedded tumor sections. Histopathologic analyses with anti-E-cadherin, anti-CD31 and anti-Ki67 IgG were also performed, using Universal ABC detection kit (Vector). The sections were examined under Olympus Provis AX70 microscope connected to a Nikon camera.

2.13. HPLC analysis of VCN-2 in serum

Mice (n=3) were administered either 0.1 ml corn oil or 25 μ g VCN-2/mice (1 mg/kg b.w.) by oral gavage on alternate days for 8 weeks. On the last day, blood was collected within 1 h after final dosage. The 100 μ l of serum was subjected to protein precipitation using 200 μ l of methanol and vortexed for 1 min. The sample was centrifuged at 13300 rpm for 15 min at 4 $^{\circ}$ C and the clear supernatant was lyophilized and dissolved in 200 μ l of methanol: 0.2% phosphoric acid buffer (58:42 v/v). The 25 μ l of sample was subjected to HPLC analysis using C₁₈ column at wavelength of 295 nm on Agilent 1100 system with auto injector (Agilent Technologies, CA). The mobile phase consisted of acetonitrile (ACN) and water at a flow rate of 1.0 ml/min with following gradient: 0-1 min: ACN-10%, H₂O-90% ; 1-2 min: gradually increasing to ACN-20%, H₂O-80% ; 2-14 min: gradually changing to ACN-90%, H₂O-10% ; 14-16 min: ACN-10%, H₂O-90%.

2.14. Statistical Analyses

Each experiment was repeated at least twice to ensure reproducibility of the results. All data were evaluated with a two-tailed unpaired student's t test are expressed as the mean \pm SD. Changes in tumor size and body weight during the course of the experiments were

visualized by scatter plot. The statistical significance of differences between control and treatment groups was determined by ANOVA followed by multiple comparison tests. Differences were considered statistically significant when the *P* value was less than 0.05. Synergism, additive effects, or antagonism were assessed by the Chou-Talalay method. In this method, CI was used to express synergism (CI less than 1), an additive effect (CI equal to 1) or antagonism (CI greater than 1).

3. Results

3.1. Anti-proliferative and pro-apoptotic effect of VCN-2 in CaP

We performed preliminary screening of the *OSL* flavonoids, VCN-2 and orientin, along with luteolin, a common flavonoid being investigated for potential CaP targeted interventions [29,30]. VCN-2 was effective in decreasing the survival of both androgen-dependent and androgen-independent CaP sparing normal PREC cells {[IC₅₀ for VCN-2 at 72h: androgen-dependent CaP (LNCaP): 44±3 μM, Androgen-independent CaP (PC3 and DU145): 25±3 μM], [IC₅₀ for luteolin at 72h: LNCaP: 78±6 μM, PC3 and DU145: 53±4 μM], [IC₅₀ for orientin at 72h: LNCaP: 124±7 μM, PC3 and DU145: 104±7 μM]}. Cell survival analysis by MTT assay revealed that VCN-2 is the most potent among the three flavonoids tested in CaP (**Supplementary Table 1**). VCN-2 was more potent in inhibiting the clonogenic potential of CaP in colony forming assay when compared to luteolin and orientin without affecting the normal PREC cells (**Fig 1A**). We next investigated the detailed mechanisms of action of VCN-2 in LNCaP and PC3 cells following determination of the IC₅₀ values at 24 h [IC₅₀ 24h: LNCaP: 112±8 μM, PC3: 70±5 μM]. For further experiments, we used 50 μM of VCN-2 for 24 h treatment in both the cell lines as cell death should be minimal for mechanistic and imaging studies focused on early cellular events that contribute to eventual cytotoxicity at 72 h. The VCN-2 treatment increased caspase-3 cleavage as determined by *in situ* caspase-3 cleavage assay (**Fig 1B**: green fluorescence indicates cleaved caspase-3). Also, VCN-2 treatment induced apoptosis as determined by annexin V staining (flipping of cell membrane), TUNEL apoptotic assay (DNA fragmentation induced due to apoptosis) and Hoechst staining (chromatin clumping that marks the death of cells) (**Fig 1C**). The cytotoxicity of VCN-2 in CaP sparing normal PREC cells in MTT, clonogenic survival and apoptotic assays revealed that VCN-2 is a potential flavonoid that could have significant therapeutic relevance in targeting CaP.

3.2. VCN-2 treatment inhibits angiogenesis, migration and induces G2/M arrest

Tumors have enhanced rate of vascularization compared to surrounding normal tissues due to adaptations in tumor signaling pathways and angiogenesis has been a vital focus of developing novel agents for prostate cancer interventions [31]. Hence, we tested the impact of VCN-2 on angiogenesis *in vitro* aortic ring assay [28]. VCN-2 treatment inhibited the neo-vascular network formation around mice aorta cultured in Matrigels (**Fig 2A**). VCN-2 treatment caused significant reduction in the levels of VEGF-expression (**Fig 2B**, **p*<0.001). VCN-2 also inhibited the migration of CaP cells *in vitro* wound healing assay (**Fig 2C**). The anti-proliferative effect of VCN-2 was further examined by cell cycle FACS analysis. VCN-2 treatment caused G2/M phase arrest in both androgen-dependent and androgen-independent CaP cells (~51% cells accumulated in G2 phase) (**Fig 2D**).

3.3. VCN-2 induces apoptosis and inhibits EGFR/Akt/mTOR/ p70S6K pathway

The VCN-2 treatment enhanced the PARP-cleavage along with decreasing the levels of fibronectin, anti-apoptotic Bcl2 expression and increasing the pro-apoptotic Bax and tumor suppressor E-cadherin expression (**Fig 3A**). EGFR and PI3K/Akt/mTOR activation has been implicated in prostate cancer progression and metastasis [32,33]. VCN-2 treatment attenuated the activation of EGFR which was predominant in androgen-dependent LNCaP

cells compared to androgen-independent PC3 cells. VCN-2 decreased the pAkt (S⁴⁷³) levels in both the CaP cells. VCN-2 caused significant decrease in the activation of the mTOR signal transducer pP70S6K (S²⁴⁰⁻²⁴⁴) (**Fig 3B**).

VCN-2 treatment also caused decrease in the levels of cyclin B1, cyclin D1 and CDK4. CDK4, though usually associated with G1 transition, has been also studied for its regulatory role in G2/M transition. Over-expression of dominant negative CDK4 leads to arrest of G2 phase progression [34]. Some of the active and natural anti-cancer compounds like apigenin and thiomersal also cause inhibition of CDK4 and cyclin B1 while causing G2/M phase arrest [35,36]. VCN-2 also decreased the levels of proliferating cell nuclear antigen (PCNA) and human telomerase reverse transcriptase (hTERT) (**Fig 3C**). PTEN expression was undetectable in PC3 cells which have homozygous deletion of PTEN [37]. During proliferation of cells, phosphorylation of Rb is known to cause its functional inactivation [38,39]. VCN-2 caused decrease in the levels of pRb (S⁷⁸⁰) compared to controls which in turn would facilitate its tumor suppressor function. VCN-2 increased the levels of p53 expression in LNCaP cells and enhanced p21 levels in both LNCaP and PC3 cells. Regulation of p21 can be p53-dependent and p53-independent [40]. The p21 protein regulation is mediated by both p53 and C-Myc where p53 positively regulates p21 and CMyc negatively regulates p21 transcription [40,41]. The down-regulation of c-Myc by VCN-2 treatment would explain the up-regulation of p21 in the p53-null PC3 cells [41] (**Fig 3D**).

We next performed signaling network analysis by employing the bioinformatic software “Ingenuity pathway analysis” (IPA) using the ratios obtained from the average of densitometric values from Western-blot analyses. IPA analysis revealed that VCN-2 significantly regulates the network of cancer and cell development (**Supplementary Fig 1**). The major activating signaling nodes in the interconnected network are down-regulated by VCN-2 (green) where as major tumor inhibitory signaling nodes like p21 or cyclin-dependent kinase inhibitor 1A (CDKN1A) are up-regulated by VCN-2 (red). Thus, the impact of VCN-2 on different signaling proteins does not merely indicate diffuse anti-cancer signaling effects at individual protein levels, but represents a collective inhibitory effect at a higher network level. The coherent inhibition of a vital cancer network represents a much stronger anti-tumor potential of a candidate drug than only regulating few single proteins of different networks in general. The IPA analysis also revealed the statistically significant impact of VCN-2 on major pathways including prostate cancer signaling, cell morphology, aryl hydrocarbon receptor signaling along with connective tissue development and function which regulates cellular homing and migration (**supplementary Fig 1**).

The oral administration of DTL, the current drug of choice in the management of advanced androgen-independent CaP, is associated with dose-limiting complications and emergence of resistance over time [19,42]. In this regard, given the ability to VCN-2 to affect cell cycle progression and its ability to regulate key cancer signaling network, we further tested the impact of VCN-2 and DTL co-treatment *in vitro* on the survival and colony-forming ability of CaP cells.

3.4. VCN-2 and DTL induce synergistic inhibitory effect in CaP

We first performed DTL cytotoxicity by MTT assay [IC₅₀ at 72h: androgen-dependent CaP (LNCaP): 21±3 nM, androgen-independent CaP (PC3 and DU145): 33±4 nM]. Based on the cytotoxicity of VCN-2 and DTL, we further tested the effect of co-treatment of VCN-2 and DTL at lower cytotoxic concentrations of each of the drugs so that the degree of increase in cytotoxicity due to co-administration of both agents can be well characterized. VCN-2 and DTL co-treatment had a synergistic impact in causing significant decrease in the survival of CaP cells (CI<1, Chou-Talalay test, p<0.001, **Fig 4A**). VCN-2 and DTL induced

synergistic inhibition of the clonogenic potential of CaP cells in colony-forming assay (CI<1, Chou-Talalay test, $p<0.004$, **Fig 4B**). The progression of CaP after medical or surgical castration is mediated by both androgen-dependent and androgen-independent signaling mechanisms like increase in the expression of androgen receptor (AR) and activation of alternate signaling pathways like insulin growth factor 1 receptor (IGF-1R) [10,43]. Hence, we investigated the effect of VCN-2 alone and in combination with DTL on AR in AR expressing LNCaP cells as PC3 cells do not express AR. Our results revealed that VCN-2 alone causes down-regulation of AR and potentiates the DTL-induced decrease in AR levels (**Fig 4C**: lane 11 vs. lanes 2 and 6). We further sought to characterize the effect of VCN-2 on regulating IGF-1R signaling which can provide additional rationale for the use of VCN-2 in androgen-independent PC3 cells [10, 44]. VCN-2 effectively down-regulated both the constitutive and IGF1 induced activation of IGF-1R (Y¹¹³¹) and downstream pAkt (S⁴⁷³). Thus, the inhibition of pIGF1R (Y¹¹³¹) represents an important mechanism of action of VCN-2 contributing to its anti-cancer effects in androgen-independent CaP cells (**Fig 4D**).

The results from *in vitro* studies provided strong evidence and mechanistic rationale for the synergistic inhibitory effect of VCN-2 and DTL in CaP cells. DTL is an anti-mitotic taxane that is administered *i.v.* once in three weeks on a ten cycle regimen along with 5 mg of prednisone twice daily in androgen-independent CaP [45]. Hence, we performed *in vivo* mice xenograft studies with VCN-2 and DTL by oral route of administration on alternate days.

3.5. The effect of VCN-2 alone and in combination with DTL on tumor regression in vivo mice xenografts

VCN-2 administration on alternated days by oral gavage induced potent regression of tumors *in vivo* whereas uncontrolled growth was observed in the animals treated with vehicle (corn oil) only. At day 60, tumor cross-sectional area and tumor-weight of mice bearing PC3 cells was significantly lower in VCN-2 (1 mg/kg equivalent to 0.0001% w/w) treated group as compared to the vehicle treated group ($54.5 \pm 6 \text{ mm}^2$ vs. $128 \pm 11 \text{ mm}^2$; $p<0.001$ and $0.89 \pm 0.11 \text{ g}$ vs. $1.85 \pm 0.24 \text{ g}$; $p<0.01$, respectively; $n=5$). In parallel, at day 60, tumor cross-sectional area and tumor-weight of mice bearing PC3 cells was significantly lower in DTL (0.01 mg/kg equivalent to 0.000001% w/w) treated group as compared to the vehicle treated group ($43.6 \pm 6 \text{ mm}^2$ vs. $128 \pm 11 \text{ mm}^2$; $p<0.001$ and $0.75 \pm 0.12 \text{ g}$ vs. $1.85 \pm 0.24 \text{ g}$; $p<0.001$, respectively; $n=5$). The combination of VCN-2 (1 mg/kg) and DTL (0.01 mg/kg) induced synergistic effect with significant tumor regression and reduction in tumor-weight as compared to the vehicle treated group [$25.8 \pm 3 \text{ mm}^2$ vs. $128 \pm 11 \text{ mm}^2$ and $0.17 \pm 0.03 \text{ g}$ vs. $1.85 \pm 0.24 \text{ g}$; respectively, CI <1 (Chou-Talalay test), $p<0.001$, $n=5$]. Alternate day oral administration of DTL along with VCN-2 was highly effective and tolerable without any overt toxicity (**Fig 5 and supplementary Fig 2**).

3.6. Impact of VCN-2 and DTL on the tumor signaling proteins

The histopathological examination of paraffin-embedded tumor xenograft sections by H&E staining revealed that VCN-2 reduces the number of tumor blood vessels and restores the normal morphology when compared to controls (**Fig 6A**). VCN-2 alone decreased the levels of proliferation marker, Ki67 and angiogenesis marker, CD31 which was further decreased by co-administration of VCN-2 and DTL [46]. VCN-2 alone and in combination with DTL, up-regulated the expression of E-cadherin. E-cadherin is a suppressor of invasion and growth of many cancers because of its role in the inhibition of epithelial-mesenchymal transition (EMT) and promoting normal differentiation [47,48]. E-cadherin is frequently down-regulated during prostate cancer progression and correlates with poor prognosis [12, 49]. In this regard, enhanced over-expression of E-cadherin consequent to VCN-2 and DTL

treatment represents a highly significant and novel mechanism of action that contributes to normal differentiation of prostate tumors in the treated groups (**Fig 6A**).

Following *in vivo* tumor regression and histopathological analysis, we further analyzed the effect of VCN-2 alone and in combination with DTL on critical signaling nodes of importance in prostate cancer by Western-blot analysis of tumor tissue lysates. The PARP-cleavage, a marker of apoptosis, was evident in VCN-2 treated groups which was further enhanced with DTL co-administration. VCN-2 decreased pAkt, pRb, PCNA, cyclin D1, fibronectin, IGF-1R levels which were further down-regulated with VCN-2 and DTL combinatorial treatment. The activation of E-cadherin expression consequent to VCN-2 and DTL treatment as revealed by initial histopathological examination of tumor sections was also validated by Western-blot analysis (**Fig 6B**).

3.7. VCN-2 concentration in mice serum after oral administration

Following mice xenograft studies, we next determined the levels of VCN-2 in serum after oral dosage. The extent of absorption of VCN-2 was studied by analyzing the serum samples of mice treated with 25 µg/mice (1 mg/kg b.w.) of VCN-2 on alternate days for 8 weeks by reversed-phase HPLC. VCN-2 was effectively absorbed after oral dosage reaching a concentration of 2.6 ± 0.3 µmol/L in serum as determined by HPLC analysis. We only identified the VCN-2 but not the metabolites of VCN-2. Many flavonoids are metabolized rapidly after oral administration and thus the detectable free forms of the drug in serum are minimal. In this regard, our studies provide “proof-of-concept” evidence that orally administered VCN-2 is absorbed in to the serum. The further detailed studies on short term and long term absorption, distribution, metabolism and excretion (ADME) pharmacokinetics of VCN-2 and its metabolites when administered alone as well as in combination with DTL is being currently underway in our laboratory.

4. Discussion

In spite of rapid advances in translational research, the management of CaP is still associated with substantial challenges considering the molecular complexity of primary pathogenesis and recurrence of refractory androgen-independent CaP following initial hormonal therapy [50]. The advanced and metastatic CaP is still a major clinical challenge which is associated with a poor 5 year survival rate of 30.2%. The incidence/mortality rate of CaP is substantially high at 8.1 which translate in to that CaP is the cause of death in approximately 1 in 8 affected men [1]. Hence, the characterization of novel anti-cancer agents is of potential relevance to address contemporary challenges in the management of CaP.

The VCN-2 treatment was effective in inhibiting proliferation and migration of both androgen-dependent and androgen-independent CaP. VCN-2 alone down-regulated AR, C-Myc, pIGF-1R, fibronectin, mTOR signal transducer pP70S6K, hTERT, pRb, Bcl2, PCNA, cell cycle regulators like cyclin B1 and cyclin D1 levels while increasing pro-apoptotic Bax, tumor suppressors like p53 and E-cadherin which are of specific relevance to both primary pathogenesis and emergence of androgen-independent CaP (6-12). Importantly, VCN-2 inhibited IGF1/IGF1R pathway which is important for androgen-independent CaP survival and progression [10]. Mice xenograft studies confirmed that oral administration of VCN-2 is effective in causing tumor regression along with inducing anti-tumor signaling as observed *in vitro* studies. VCN-2 alone induced potent anti-angiogenic effect which was confirmed by both *in vitro* aortic ring assay and histopathological examination of resected tumors from *in vivo* mice xenograft studies.

DTL is the FDA approved drug of choice in the management of metastatic androgen-independent CaP and has contributed to improved survival and quality of life in patients

suffering with metastatic CaP. The *i.v.* administration of DTL is associated with substantial toxicities as single dose administration of DTL, an anti-mitotic taxane, is associated with adverse effects arising from direct exposure to rapidly dividing cells in bone marrow which in turn results in febrile neutropenia and anemia [19-22]. Generally, oral DTL administration alone leads to less bioavailability compared to *i.v.* administration. Our *in vitro* studies initially revealed synergistic effect due to VCN-2 and DTL. Hence, for *in vivo* studies, given the current focus of developmental therapeutics research on alternate routes of DTL administration, we focused on oral route of DTL which turned out to be effective. The oral DTL and VCN-2 administration induced potent synergistic effect which was characterized by significant decrease in AR, pIGF-1R and pAkt levels among effects on other signaling cascades as revealed by our studies. The salient feature of this study was the potent synergistic effect of VCN-2 and a low dose of DTL (0.03 mg/m² of DTL and 3 mg/m² of VCN-2 orally on alternate days compared to clinical dose in metastatic androgen-independent CaP: 75 mg/m² of DTL *i.v.* once in 3 wks. plus 5 mg prednisone twice daily) which strongly supports further development of VCN-2 and DTL combinatorial regimens for clinical use in aggressive cases of androgen-independent CaP. Flavonoids can modulate the drug action by multiple mechanisms like influencing intestinal absorption, altering rate and nature of metabolism, biodistribution of the drug and most importantly impacting parallel signaling networks in targeted cancers when co-administered with chemotherapy drugs resulting in additive, antagonistic or synergistic effects. Further detailed pharmacokinetic studies would reveal the extensive mechanisms that contribute to differences in absorption and metabolism of VCN-2 and DTL that could be complementing to observed effects on tumor signaling effects as revealed by our current studies.

Our *in vivo* mice xenograft studies further accommodated the desired criteria of altered route of administration of DTL by using oral gavage during DTL and VCN-2 co-administration. The results from *in vivo* studies revealed that oral administration of DTL and VCN-2 is effective and tolerable along with providing corroborative evidence to the synergistic anti-tumor effects as observed by initial *in vitro* studies. The VCN-2 and DTL co-administration caused greater decrease in the levels of proliferation marker, Ki67 and angiogenic marker, CD31 while increasing the tumor suppressor E-cadherin expression to a greater extent than either of the agents alone. VCN-2 and DTL enhanced the levels of total Rb while decreasing the levels of functionally inactive of pRb (S⁷⁸⁰) more effectively. The further mechanistic evidence for the synergistic effect of VCN-2 and DTL combination was provided by the enhanced inhibition of critical signaling proteins like pAkt (S⁴⁷³), pIGF-1R, PCNA, cyclin D1 and fibronectin following co-administration than as single agents.

In summary, our results revealed the ability of novel flavonoid VCN-2 to recalibrate cellular oncogenic, tumor suppressor and differentiation signaling cascades to induce multi-specific anti-cancer effects of specific relevance to the critical nodes of pathogenesis of CaP which collectively provide strong rationale for further studies on developing VCN-2 for prostate cancer interventions. The results from this preclinical study which provide both *in vitro* and *in vivo* evidence to the synergistic tumor regression due to oral DTL and VCN-2 combination have unveiled a potential DTL combinatorial regimen for further clinical development towards the management of metastatic androgen-independent carcinoma of prostate.

Supplementary Material

Refer to Web version on PubMed Central for supplementary material.

Acknowledgments

This work was supported in part by USPHS grant CA 77495 and the Cancer Research Foundation of North Texas. We sincerely thank our ongoing collaborator Dr. Laszlo Prokai, Robert A Welch Chair in Biochemistry (supported by the Welch Foundation endowment BK-0031) at UNTHSC for providing the access to Ingenuity pathway analysis (IPA). We also thank Dr. Sumihiro Suzuki, Department of Biostatistics, School of Public Health, UNTHSC, Fort Worth, TX, for his assistance in the statistical analyses of the data.

The abbreviations used are

CaP	Carcinoma of prostate
VCN-2	vicenin-2
DTL	docetaxel
PCNA	proliferating cell nuclear antigen
AR	androgen receptor

References

1. Surveillance, Epidemiology, and End Results (SEER) Program (www.seer.cancer.gov) Research Data (1973-2008), National Cancer Institute, DCCPS, Surveillance Research Program, Cancer Statistics Branch, released April 2011, based on the November 2010 submission.
2. Andreoiu M, Cheng L. Multifocal prostate cancer: Biologic, prognostic, and therapeutic implications. *Hum. Pathol.* 2010; 41:781–93. [PubMed: 20466122]
3. Tomlins SA, Mehra R, Rhodes DR, Cao X, Wang L, Dhanasekaran SM, et al. Integrative molecular concept modeling of prostate cancer progression. *Nat. Genet.* 2007; 39:41–51. [PubMed: 17173048]
4. Lee MC, Moussa AS, Yu C, Kattan MW, Magi-Galluzzi C, Jones JS. Multi-focal high grade prostatic intraepithelial neoplasia is a risk factor for subsequent prostate cancer. *J Urol.* 2010; 184:1958–62. [PubMed: 20846692]
5. Delacroix SE, Ward JF. Prostate cancer multifocality: Impact on cancer biology and treatment recommendations. *Panminerva Med.* 2010; 52:209–16. [PubMed: 21045777]
6. Abate-Shen C, Shen MM. Molecular genetics of prostate cancer. *Genes Dev.* 2010; 14:2410–34. [PubMed: 11018010]
7. Ellwood-Yen K, Graeber TG, Wongvipat J, Iruela-Arispe ML, Zhang J, Matusik R, et al. Myc-driven murine prostate cancer shares molecular features with human prostate tumors. *Cancer Cell.* 2003; 4:223–38. [PubMed: 14522256]
8. Wang S, Gao J, Lei Q, Rozengurt N, Pritchard C, Jiao J, et al. Prostate-specific deletion of the murine pten tumor suppressor gene leads to metastatic prostate cancer. *Cancer Cell.* 2003; 4:209–21. [PubMed: 14522255]
9. Sharma A, Yeow WS, Ertel A, Coleman I, Clegg N, Thangavel C, et al. The retinoblastoma tumor suppressor controls androgen signaling and human prostate cancer progression. *J Clin Invest.* 2010; 120:4478–92. [PubMed: 21099110]
10. Chan JM, Stampfer MJ, Ma J, Gann P, Gaziano JM, Pollak M, et al. Insulin-like growth factor-I (IGF-I) and IGF binding protein-3 as predictors of advanced-stage prostate cancer. *J Natl Cancer Inst.* 2002; 94:1099–106. [PubMed: 12122101]
11. McDonnell TJ, Troncoso P, Brisbay SM, Logothetis C, Chung LW, Hsieh JT, et al. Expression of the protooncogene bcl-2 in the prostate and its association with emergence of androgen-independent prostate cancer. *Cancer Res.* 1992; 52:6940–4. [PubMed: 1458483]
12. van Oort IM, Tomita K, van Bokhoven A, Bussemakers MJ, Kiemeny LA, Karthaus HF, et al. The prognostic value of E-cadherin and the cadherin-associated molecules alpha-, beta-, gamma-catenin and p120ctn in prostate cancer specific survival: A long-term follow-up study. *Prostate.* 2007; 67:1432–8. [PubMed: 17639504]

13. Singh S, Majumdar DK, Rehan HM. Evaluation of anti-inflammatory potential of fixed oil of *ocimum sanctum* (holybasil) and its possible mechanism of action. *J Ethnopharmacol.* 1996; 54:19–26. [PubMed: 8941864]
14. Rai V, Iyer U, Mani UV. Effect of tulasi (*ocimum sanctum*) leaf powder supplementation on blood sugar levels, serum lipids and tissue lipids in diabetic rats. *Plant Foods Hum Nutr.* 1997; 50:9–16. [PubMed: 9198110]
15. Trush MA, Kensler TW. An overview of the relationship between oxidative stress and chemical carcinogenesis. *Free Radic Biol Med.* 1991; 10:201–9. [PubMed: 1864525]
16. Sabichi AL, Lippman SM. COX-2 inhibitors and other non-steroidal anti-inflammatory drugs in genitourinary cancer. *Semin Oncol.* 2004; 31:36–44. [PubMed: 15179622]
17. Singh RP, Sharma G, Dhanalakshmi S, Agarwal C, Agarwal R. Suppression of advanced human prostate tumor growth in athymic mice by silibinin feeding is associated with reduced cell proliferation, increased apoptosis, and inhibition of angiogenesis. *Cancer Epidemiol Biomarkers Prev.* 2003; 12:933–9. [PubMed: 14504208]
18. Karthikeyan K, Ravichandran P, Govindasamy S. Chemopreventive effect of *ocimum sanctum* on DMBA-induced hamster buccal pouch carcinogenesis. *Oral Oncol.* 1999; 35:112–9. [PubMed: 10211319]
19. Engels FK, Verweij J. Docetaxel administration schedule: From fever to tears? A review of randomised studies. *Eur J Cancer.* 2005; 41:1117–26. [PubMed: 15911234]
20. Petrylak DP. Future directions in the treatment of androgen-independent prostate cancer. *Urology.* 2005; 65:8–12. [PubMed: 15939077]
21. Oudard S, Legrier ME, Boye K, Bras-Goncalves R, De Pinieux G, De Cremoux P, et al. Activity of docetaxel with or without estramustine phosphate versus mitoxantrone in androgen dependent and independent human prostate cancer xenografts. *J Urol.* 2003; 169:1729–34. [PubMed: 12686819]
22. Beer TM, Ryan CW, Venner PM, Petrylak DP, Chatta GS, Ruether JD, et al. Double-blinded randomized study of high-dose calcitriol plus docetaxel compared with placebo plus docetaxel in androgen-independent prostate cancer: A report from the ASCENT investigators. *J Clin Oncol.* 2007; 25:669–74. [PubMed: 17308271]
23. Singhal J, Singhal SS, Yadav S, Suzuki S, Warnke MM, Yacoub A, et al. RLIP76 in defense of radiation poisoning. *Int J Radiat Oncol Biol Phys.* 2008; 72:553–61. [PubMed: 18793957]
24. Baskin DS, Ngo H, Didenko VV. Thimerosal induces DNA breaks, caspase-3 activation, membrane damage, and cell death in cultured human neurons and fibroblasts. *Toxicol Sci.* 2003; 74:361–8. [PubMed: 12773768]
25. Singhal SS, Yadav S, Vatsyayan R, Chaudhary P, Borvak J, Singhal J, et al. Increased expression of *cdc2* inhibits transport function of RLIP76 and promotes apoptosis. *Cancer Lett.* 2009; 283:152–8. [PubMed: 19375851]
26. Singhal SS, Yadav S, Drake K, Singhal J, Awasthi S. Hsf-1 and POB1 induce drug sensitivity and apoptosis by inhibiting *Ralbp1*. *J Biol Chem.* 2008; 283:19714–29. [PubMed: 18474607]
27. Xiang N, Zhao R, Zhong W. Sodium selenite induces apoptosis by generation of superoxide via the mitochondrial-dependent pathway in human prostate cancer cells. *Cancer Chemother Pharmacol.* 2009; 63:351–62. [PubMed: 18379781]
28. Yi T, Yi Z, Cho SG, Luo J, Pandey MK, Aggarwal BB, et al. Gambogic acid inhibits angiogenesis and prostate tumor growth by suppressing vascular endothelial growth factor receptor 2 signaling. *Cancer Res.* 2008; 68:1843–50. [PubMed: 18339865]
29. Devi PU, Bisht KS, Vinitha M. A comparative study of radioprotection by *ocimum* flavonoids and synthetic aminothiols protectors in the mouse. *Br J Radiol.* 1998; 71:782–4. [PubMed: 9771390]
30. Fang J, Zhou Q, Shi XL, Jiang BH. Luteolin inhibits insulin-like growth factor 1 receptor signaling in prostate cancer cells. *Carcinogenesis.* 2007; 28:713–23. [PubMed: 17065200]
31. Yu EM, Jain M, Aragon-Ching JB. Angiogenesis inhibitors in prostate cancer therapy. *Discov Med.* 2010; 10:521–30. [PubMed: 21189223]
32. Marks RA, Zhang S, Montironi R, McCarthy RP, MacLennan GT, Lopez-Beltran A, et al. Epidermal growth factor receptor (EGFR) expression in prostatic adenocarcinoma after hormonal therapy: A fluorescence in situ hybridization and immunohistochemical analysis. *Prostate.* 2008; 68:919–23. [PubMed: 18409189]

33. Gao N, Zhang Z, Jiang BH, Shi X. Role of PI3K/AKT/mTOR signaling in the cell cycle progression of human prostate cancer. *Biochem Biophys Res Commun.* 2003; 310:1124–32. [PubMed: 14559232]
34. Gabrielli BG, Sarcevic B, Sinnamon J, Walker G, Castellano M, Wang XQ, et al. A cyclin D-Cdk4 activity required for G2 phase cell cycle progression is inhibited in ultraviolet radiation-induced G2 phase delay. *J Biol Chem.* 1999; 274:13961–9. [PubMed: 10318807]
35. Yin F, Giuliano AE, Law RE, Van Herle AJ. Apigenin inhibits growth and induces G2/M arrest by modulating cyclin-CDK regulators and ERK MAP kinase activation in breast carcinoma cells. *Anticancer Res.* 2001; 21:413–20. [PubMed: 11299771]
36. Woo KJ, Lee TJ, Bae JH, Jang BC, Song DK, Cho JW, et al. Thimerosal induces apoptosis and G2/M phase arrest in human leukemia cells. *Mol Carcinog.* 2006; 45:657–66. [PubMed: 16649253]
37. Festuccia C, Muzi P, Millimaggi D, Biordi L, Gravina GL, Specca S, et al. Molecular aspects of gefitinib antiproliferative and pro-apoptotic effects in PTEN-positive and PTEN-negative prostate cancer cell lines. *Endocr. Relat. Cancer.* 2005; 12:983–98. [PubMed: 16322337]
38. Schmitz NM, Hirt A, Aebi M, Leibundgut K. Limited redundancy in phosphorylation of retinoblastoma tumor suppressor protein by cyclin-dependent kinases in acute lymphoblastic leukemia. *Am J Pathol.* 2006; 169:1074–9. [PubMed: 16936279]
39. Tyagi A, Agarwal C, Agarwal R. Inhibition of retinoblastoma protein (rb) phosphorylation at serine sites and an increase in rb-E2F complex formation by silibinin in androgen-dependent human prostate carcinoma LNCaP cells: Role in prostate cancer prevention. *Mol Cancer Ther.* 2002; 1:525–32. [PubMed: 12479270]
40. Macleod KF, Sherry N, Hannon G, Beach D, Tokino T, Kinzler K, et al. p53-dependent and independent expression of p21 during cell growth, differentiation, and DNA damage. *Genes Dev.* 1995; 9:935–44. [PubMed: 7774811]
41. Gartel AL, Ye X, Goufman E, Shianov P, Hay N, Najmabadi F, et al. Myc represses the p21^(WAF1/CIP1) promoter and interacts with Sp1/Sp3. *Proc Natl Acad Sci.* 2001; 98:4510–5. [PubMed: 11274368]
42. Makarovskiy AN, Siryaporn E, Hixson DC, Akerley W. Survival of docetaxel-resistant prostate cancer cells in vitro depends on phenotype alterations and continuity of drug exposure. *Cell Mol Life Sci.* 2002; 59:1198–211. [PubMed: 12222966]
43. Mao HL, Zhu ZQ, Chen CD. The androgen receptor in hormone-refractory prostate cancer. *Asian J Androl.* 2009; 11:69–73. [PubMed: 19050686]
44. Floryk D, Huberman E. Differentiation of androgen-independent prostate cancer PC-3 cells is associated with increased nuclear factor-kappaB activity. *Cancer Res.* 2005; 65:11588–96. [PubMed: 16357169]
45. Petrylak DP, Tangen CM, Hussain MH, Lara PN, Jones JA, Taplin ME, et al. Docetaxel and estramustine compared with mitoxantrone and prednisone for advanced refractory prostate cancer. *N Engl J Med.* 2004; 351:1513–20. [PubMed: 15470214]
46. Scholzen T, Gerdes J. The Ki-67 protein: from the known and the unknown. *J Cell Physiol.* 2000; 182:311–22. [PubMed: 10653597]
47. Wheelock MJ, Johnson KR. Cadherins as modulators of cellular phenotype. *Annu Rev. Cell Dev Biol.* 2003; 19:207–35. [PubMed: 14570569]
48. Yang J, Weinberg RA. Epithelial-mesenchymal transition: at the crossroads of development and tumor metastasis. *Dev Cell.* 2008; 14:818–29. [PubMed: 18539112]
49. Almeida PR, Ferreira VA, Santos CC, Rocha-Filho FD, Feitosa RR, Falcao EA, et al. E-cadherin immuno-expression patterns in the characterisation of gastric carcinoma histotypes. *J Clin Pathol.* 2010; 63:635–9. [PubMed: 20591914]
50. Shen MM, Abate-Shen C. Molecular genetics of prostate cancer: New prospects for old challenges. *Genes Dev.* 2010; 24:1967–2000. [PubMed: 20844012]

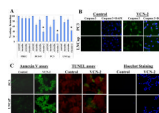


Figure 1. Anti-proliferative and pro-apoptotic effect of VCN-2 in CaP

Colony-forming assay was performed and the colonies were counted using Innotech Alpha Imager HP [23]. * $p < 0.001$ compared with control (**panel A**). For *in-situ* caspase-cleavage assay, the cells were grown on cover-slips and treated with 50 μ M VCN-2 for 24 h and caspase-cleavage was measured using APO LOGIX™ carboxyfluorescein (FAM) caspase detection kit. Activated Caspase-positive cells appeared fluorescing green and pink when co-stained with DAPI (**panel B**). For detection of early and late events of apoptosis, Annexin V staining, TUNEL apoptotic assay and Hoechst staining were performed as described in Methods. Fluorescence was examined using Zeiss LSM 510 META laser-scanning fluorescence microscope. Apoptotic cells are green in Annexin V staining (membrane flipping), in TUNEL assay (DNA breaks revealed by end labeling), green fluorescence represents apoptotic cells, whereas blue in Hoechst staining (chromatin clumping) (**panel C**).

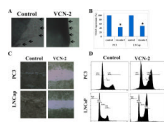


Figure 2. Effect of VCN-2 on angiogenesis, migration and cell cycle progression

The impact of VCN-2 on angiogenic sprout formation (arrows indicate borders new angiogenic vascular sprouts) in mice aortic rings cultured in Matrigels (**panel A**). VEGF-expression in control and 50 μM VCN-2 treated cells was performed by ELISA kit according to the manufacturer instructions (R&D Systems Inc., Minneapolis, MN) (**panel B**). Effect of VCN-2 on migration of LNCaP and PC3 cells in wound healing assay (**panel C**). Inhibitory effect of VCN-2 on cell cycle distribution was determined by FACS analysis. The experiment was repeated three times and similar results were obtained (**panel D**).

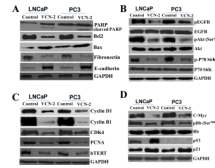


Figure 3. Effect of VCN-2 on apoptotic, proliferative and tumor suppressor proteins in CaP Androgen-dependent (LNCaP) and androgen-independent (PC3) control and 50 μ M VCN-2 treated cells were processed for Western-blot for PARP-cleavage and apoptosis regulatory proteins Bcl2 and Bax along with fibronectin and E-cadherin using specific antibodies (**panel A**). Western-blot analysis of the activation of pEGFR (Y¹⁰⁶⁸), pAkt (S⁴⁷³) and pP70S6K (S²⁴⁰⁻²⁴⁴) in LNCaP and PC3 cells following VCN-2 treatment (**panel B**). Western-blot for the levels of cell-cycle regulatory proteins cyclin B1, cyclin D1, CDK4, PCNA and hTERT (**panel C**). Western-blot for oncoprotein C-Myc, and tumor suppressors Rb, pRb (S⁷⁸⁰) p53 and p21 (**panel D**). Membranes were stripped and reprobed for GAPDH as a loading control.

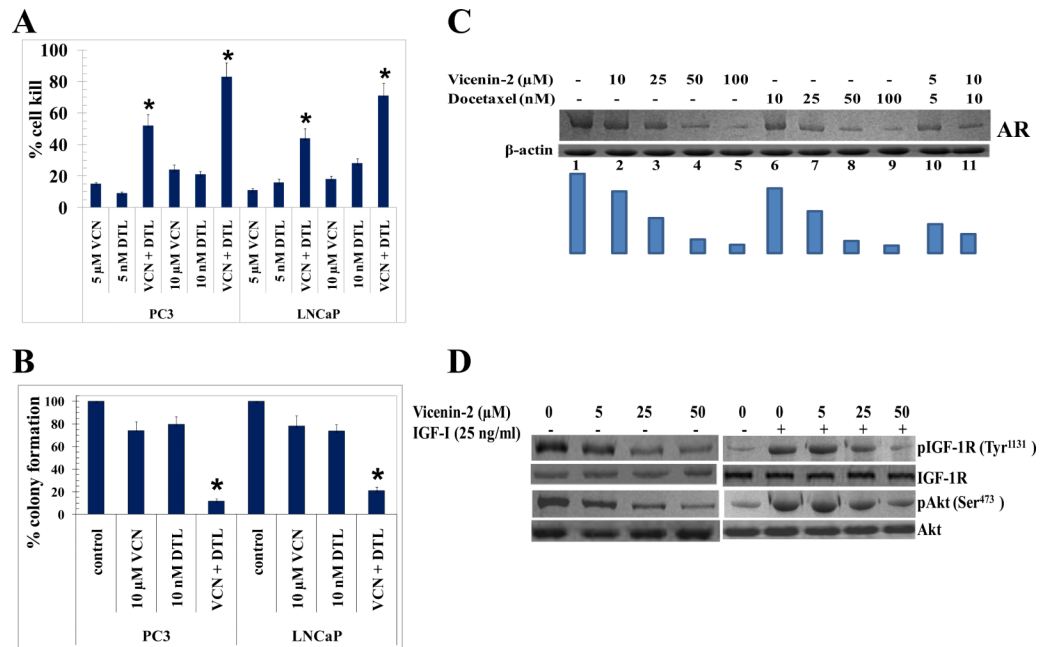


Figure 4. Effect of VCN-2 and DTL co-treatment on the survival, clonogenic potential, AR, IGF-1R and Akt activation in vitro cell cultures

The impact of VCN-2 (5 μ M and 10 μ M) and DTL (5 nM and 10 nM), alone and in combination, on the cell death as determined by MTT assay [26] (*CI<1, Chou-Talalay test, $p < 0.001$, **panel A**) and on clonogenic potential as determined by colony-formation assay (*CI<1, Chou-Talalay test, $p < 0.004$, **panel B**). Effect of VCN-2 and DTL on the regulation of AR in LNCaP cells by Western-blot against anti-AR IgG. Bars represent densitometry analysis (**panel C**). Effect of VCN-2 on IGF-1R signaling: Effect of VCN-2 on the regulation of constitutive and IGF-activated levels of pIGF1R (Y¹¹³¹) and down-stream pAkt (S⁴⁷³) in AR negative PC3 cells. The cells were incubated with indicated doses of VCN-2 for 24 h followed by incubation with 25 ng/ml IGF-1 for 30 min and subjected to immunoblotting. (**panel D**).

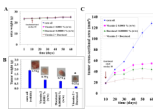


Figure 5. Effect of oral administration of VCN-2 alone and in combination with DTL on tumor regression of PC3 xenografts

The nu/nu nude mice were injected with 2×10^6 PC3 cells suspensions in 100 μ l of PBS, subcutaneously into one flank and divided in to four groups. Treatment consisted of corn oil (control), VCN-2 (1 mg/kg b.w.), DTL (0.01 mg/kg b.w.), and both, VCN-2 and DTL, in 100 μ l by oral gavage alternate day. Experimental details are given in the *Methods section*. Animals were examined daily for signs of tumor growth and body weights were recorded (**panel A**). Photographs of animals were taken at day 1, day 10, day 20, day 40, and day 60 after subcutaneous injection, are shown for all groups (*supplementary data*). Weights and photographs of tumors were also taken at day 60. * $P < 0.001$ for VCN-2 and DTL co-administration when compared to control as well as either of the single drug treatment (**panel B**). Tumors were measured in two dimensions using calipers and time-course analysis of tumor regression was performed during the study (**panel C**).

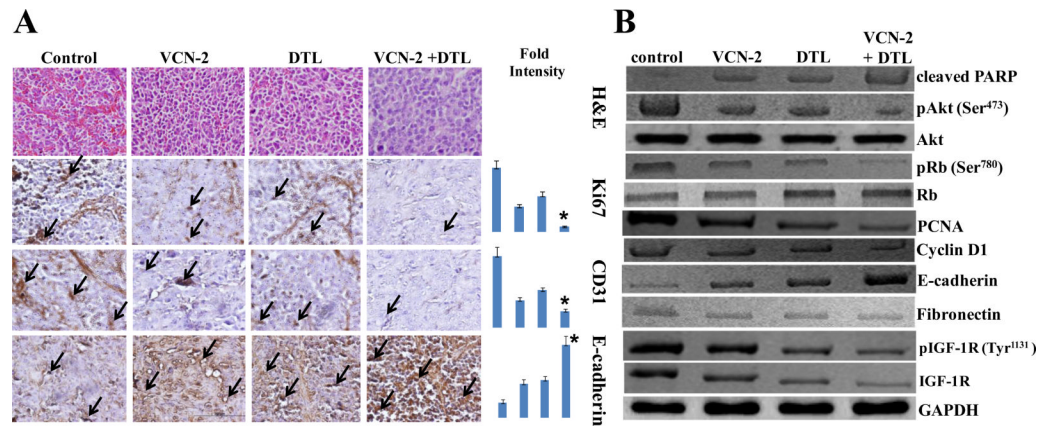


Figure 6. Histopathologic analyses of the markers of proliferation, angiogenesis and differentiation in tumor sections along with analyses of signaling proteins in tumor tissue lysates after VCN-2 treatment

Control, VCN-2 alone, DTL alone and VCN-2+DTL treated PC3 CaP bearing nude mice tumor sections were used for histopathologic analyses. Presented are H & E stained sections, IHC analyses for Ki67 expression (marker of cellular proliferation), CD31 (angiogenesis marker) and E-cadherin (tumor suppressor) from tumors in mice of control and experimental groups. Immuno-reactivity is evident as a dark brown stain. Sections were counterstained with Hematoxylin (blue). Photomicrographs at 40x magnification were acquired using Olympus Provis AX70 microscope. Percent staining was determined by measuring positive immuno-reactivity per unit area. Arrows represent the area for positive staining for an antigen. The intensity of antigen staining was quantified by digital image analysis. Statistical significance of difference was determined by two-tailed Student's *t* test. Bars represent mean \pm S.E. (n = 5); * p < 0.001 when compared to control (**panel A**). Western-blot Analysis of signaling proteins in tumor tissue lysates in control, VCN-2 alone, DTL alone as well as VCN-2 and DTL treated groups (**panel B**).